

## **EFFECT OF THE DIRECTION OF THE MAGNETIC FIELD LINES ON THE VOLTAGE OUTPUT OF A TRIBOELECTRIC NANOGENERATOR**

**El-Shazly M. H.<sup>1</sup>, Al-Kabbany A. M.<sup>2</sup> and Ali W. Y.<sup>2</sup>, Ali A. S.<sup>3</sup> and Massoud M. A.<sup>4</sup>**

<sup>1</sup>Department of Mechanical Design and Production Engineering, Faculty of Engineering, Cairo University, Giza, Egypt.

<sup>2</sup>Department of Production Engineering and Mechanical Design, Faculty of Engineering, Minia University, Minia 61111, Egypt.

<sup>3</sup>Mechanical Engineering Dept., Faculty of Engineering, Suez Canal University, EGYPT.

<sup>4</sup>Biomedical Engineering Department, Minia University, P. N. 61111, El-Minia, EGYPT.

### **ABSTRACT**

The present work investigates the effect of the direction of the magnetic field lines on the voltage output of a triboelectric nanogenerator (TENG). The effect of the permanent magnets on generation of ESC depends on the field lines relative to the triboelectrified area. The present work studies the optimal position of the permanent magnets relative to the tested area. The voltage difference between the friction surfaces of polytetrafluoroethylene (PTFE) and polyamide textile was measured after contact-separation and sliding.

Based on the experimental results, it was found that voltage increased up to maximum then decreased with further increase of the field strength when the substrate was paper sheet. The maximum voltage value was observed at certain field strength depending on the efficiency of the influence of the magnetic field on the contact area. Voltage increase was attributed to the ability of the Al electrode to cut perpendiculary the lines of a magnetic field and induce extra voltage. In contradiction to that, the sliding in the direction parallel to the field lines generated lower voltage values. Higher voltage values was displayed for rabbit fur sliding on PP than that measured for PTFE sliding on PA. Finally, it is recommended to select the proper position of the magnet to harvest the highest voltage values. The present work determined the optimal position of the permanent magnets relative to the sliding direction to get the highest voltage. This condition was realized when the moving electrode cut perpendiculary the maximum number of the lines of the magnetic field.

### **KEYWORDS**

Voltage, triboelectric nanogenerator, magnetic field lines.

### **INTRODUCTION**

When two surfaces come into contact with one another ESC can be transferred from one surface to the other, [1 - 5]. The intensity and sign of ESC is determined by the triboelectric

series that ranks materials according to their ability to obtain positive or negative ESC after contact-separation with another material, [6 - 8]. The exact mechanism of the process of triboelectrification is still unknown, [9].

Triboelectrification can cause fires, [10, 11], and damage electronics, [12, 13]. The effect of triboelectrification can be reduced by blending two materials opposite to each other in the triboelectric series in one surface, [14 - 16]. Besides, it can be used to repel viruses, [17 - 20], and make triboelectric nanogenerator (TENG), [21 - 24]. In addition to that, TENGs use a combination of triboelectrification and electrostatic induction to increase the voltage between the two terminals, where the first terminal is the dielectric connected to the electrode, and an electric ground. TENGs can be used as energy harvesters, [25 - 28], or self-powered sensors, [29 - 32]. Electromagnetic induction converts mechanical energy into electrical energy, [33 - 39].

Recently, it was found that the best results were observed for placing magnets above and under PTFE film. Finally, replacing the steel sheet by PMMA generated significant voltage increase, [40, 41]. Besides, the increase of the magnetic field caused significant voltage increase due to the ability of magnets to induce magnetic field responsible for the voltage increase.

The present work investigates the effect of the direction of the magnetic lines on the voltage generated from electromagnetic triboelectric nanogenerator (TENG).

## **EXPERIMENTAL**

The test specimens consisted of wooden cube of  $40 \times 40 \times 40 \text{ mm}^3$  coated by aluminium film (Al) of 0.25 mm thickness (first electrode). Then PTFE was adhered to the Al film representing the first dielectric surface. The tested counterface was in form of PA textile adhered to Al film of 0.1 mm thickness (second electrode) representing the second dielectric surface. The Al film was placed on 0.45 mm thick paper sheet. The voltage difference was measured between the two Al films. The counterface was replaced by polypropylene (PP) of 0.12 mm thickness and Al sheet of 0.1 mm thickness. In that condition, PTFE was replaced by rabbit fur. The details of the test specimens and test rig are shown in Fig. 1. The load was applied by the weight of the wooden block (0.5 N). The test procedure consisted of contact-separation and sliding. In contact-separation, the load is applied for 5 seconds followed by the measurement of the voltage. The sliding distance was 100 mm. The direction of sliding relative to the direction of the lines of magnetic field is shown in Fig. 2. The magnetic field was applied by permanent magnets. The intensity of the magnetic field of each magnet was 60 mG. The magnetic field was increased by using number of the magnets up to 8 magnets. Distribution of magnetic field lines is shown in Fig. 3. The experiments were repeated five times to get the voltage values.

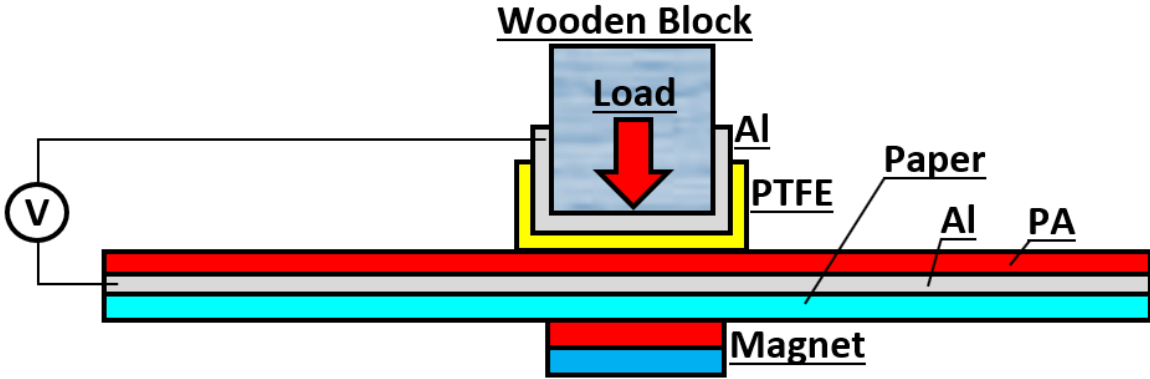


Fig. 1 Arrangement of test procedure.

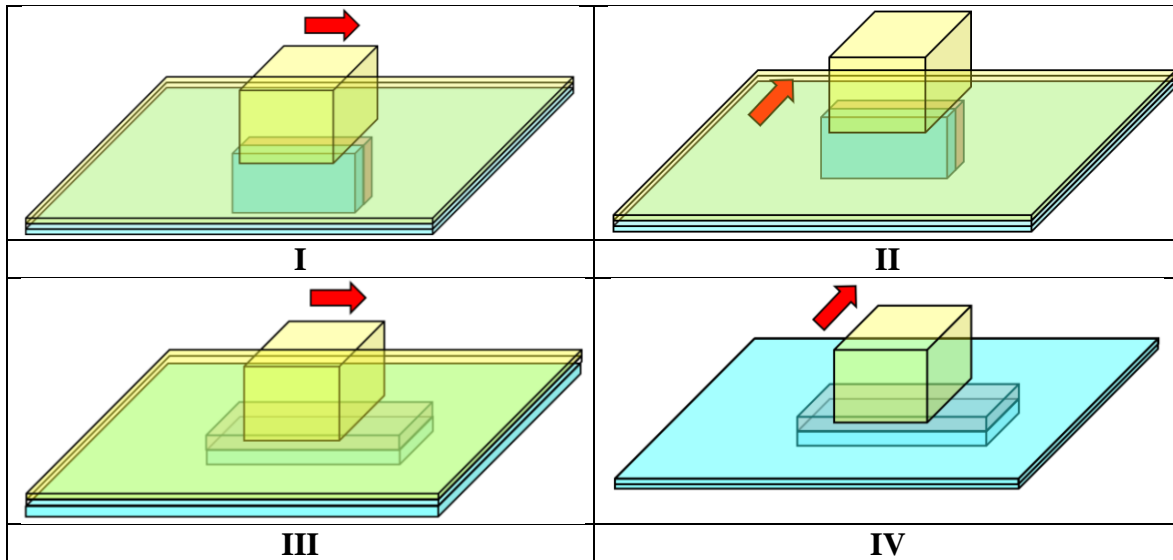


Fig. 2 The direction of sliding relative to the direction of the lines of magnetic field.

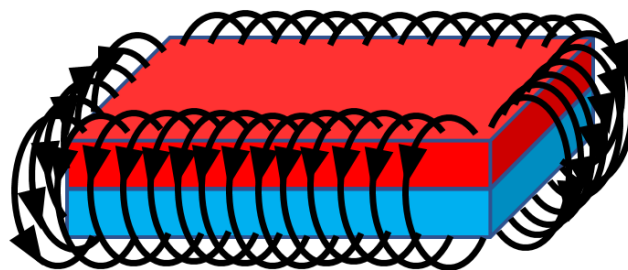
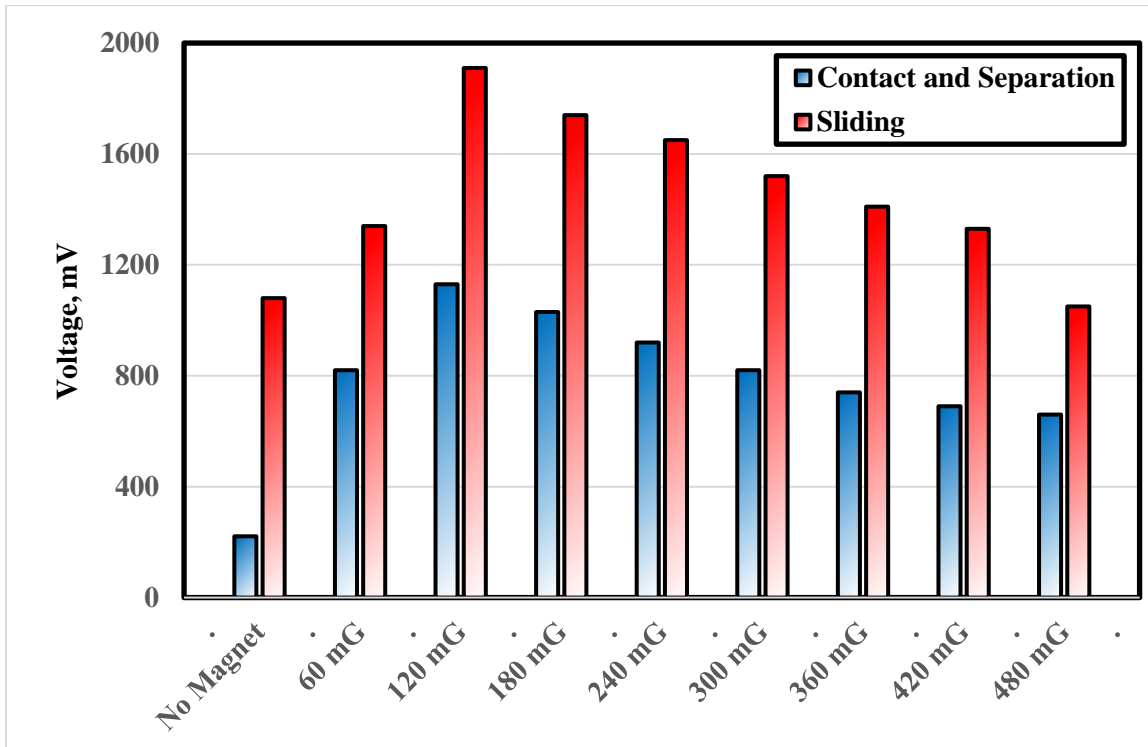


Fig. 3 Distribution of magnetic field lines.

## RESULTS AND DISCUSSION

The results of the experiments carried out to investigate the optimal direction of the magnets to get the highest ESC. Voltage generated from contact-separation and sliding when magnets were placed in the (I) position is shown in Fig. 4. Voltage difference increased significantly up to maximum at 120 mG field strength then decreased with further increase of the field

strength. The highest voltage values observed at 120 mG field strength for contact-separation and sliding were 1130 and 1910 mV respectively. Besides, voltage generated from contact-separation showed lower values than that recorded for sliding. The decrease of voltage with increasing magnetic fields may be from distribution of the magnets relative to the triboelectric area. While voltage increase may be attributed to the movement of the electrode (Al film under PTFE) that cuts across the lines of a magnetic field and induces a current that generates double layer of ESC on the contact surfaces inducing an extra electric field and leading to the voltage increase.



**Fig. 4** Voltage generated from the contact-separation and sliding of PTFE on PA, where magnets are placed in the (I) position.

When the magnets were placed in the (II) position, Fig. 5, voltage showed relatively lower values than that observed in the (I) position. This behavior can be related to the lines of magnetic field. In position (I) the Al electrode cut the field lines perpendicularly, so that the magnetic force acting on the electrode was maximum. While in position (II), the electrode moved parallel to the magnetic field leading to no change in the magnetic flux, therefore the voltage decreased. It is recommended to select the proper position of the magnet to get the highest voltage values. It is well known that, as the magnetic flux density increased, the voltage of the TENG increased. That assumption is conditioned by the proper position of the magnet. Voltage measured after sliding showed relatively higher values than that observed from contact-separation because the number of magnetic field lines cut by the movement of Al electrode increased.

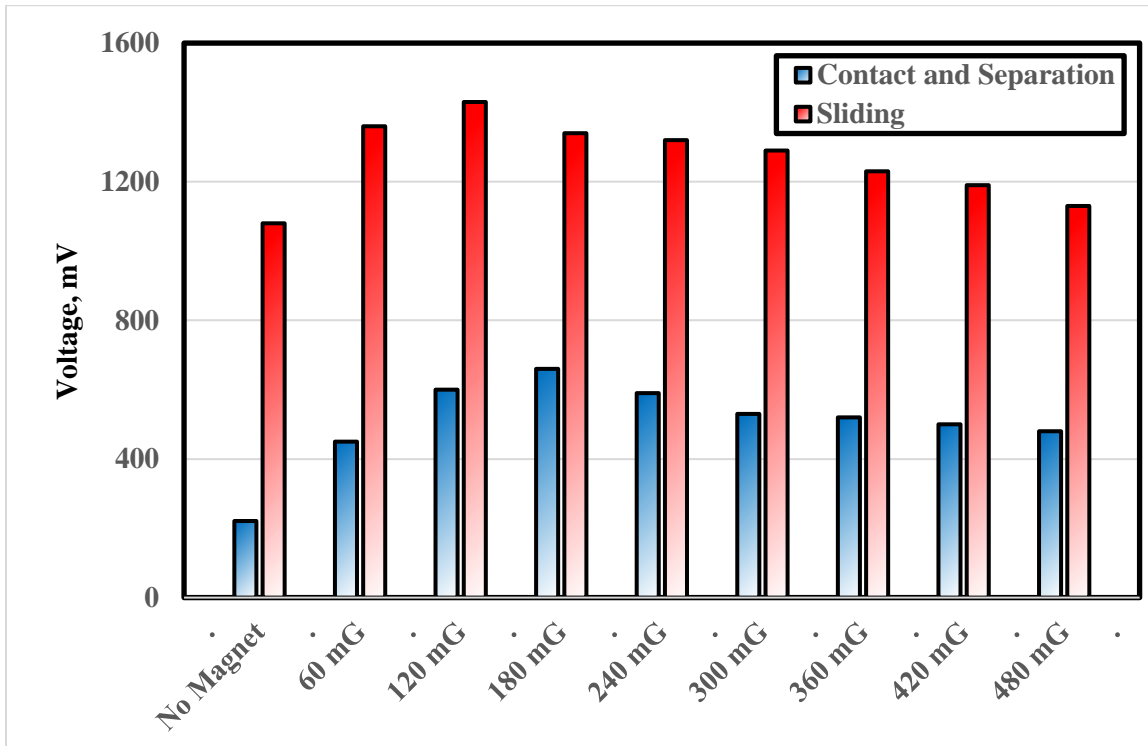


**Fig. 5** Voltage generated from the contact-separation and sliding of PTFE on PA, where magnets are placed in the (II) position.

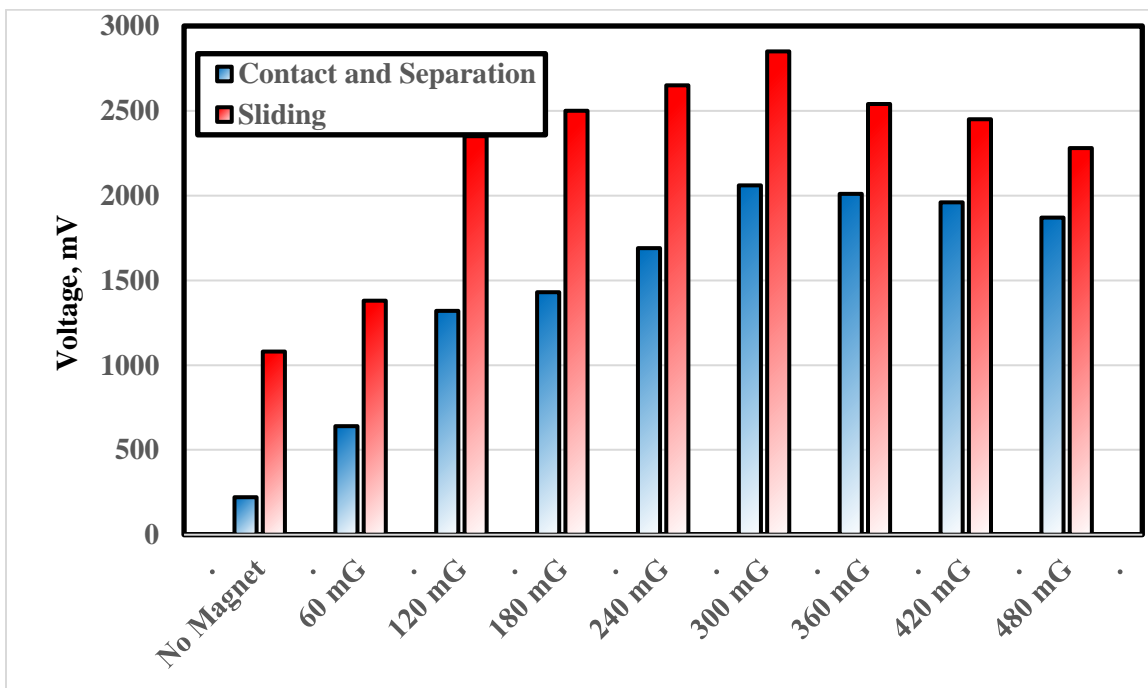


**Fig. 6** Voltage generated from the contact-separation and sliding of PTFE on PA, where magnets are placed in the (III) position.

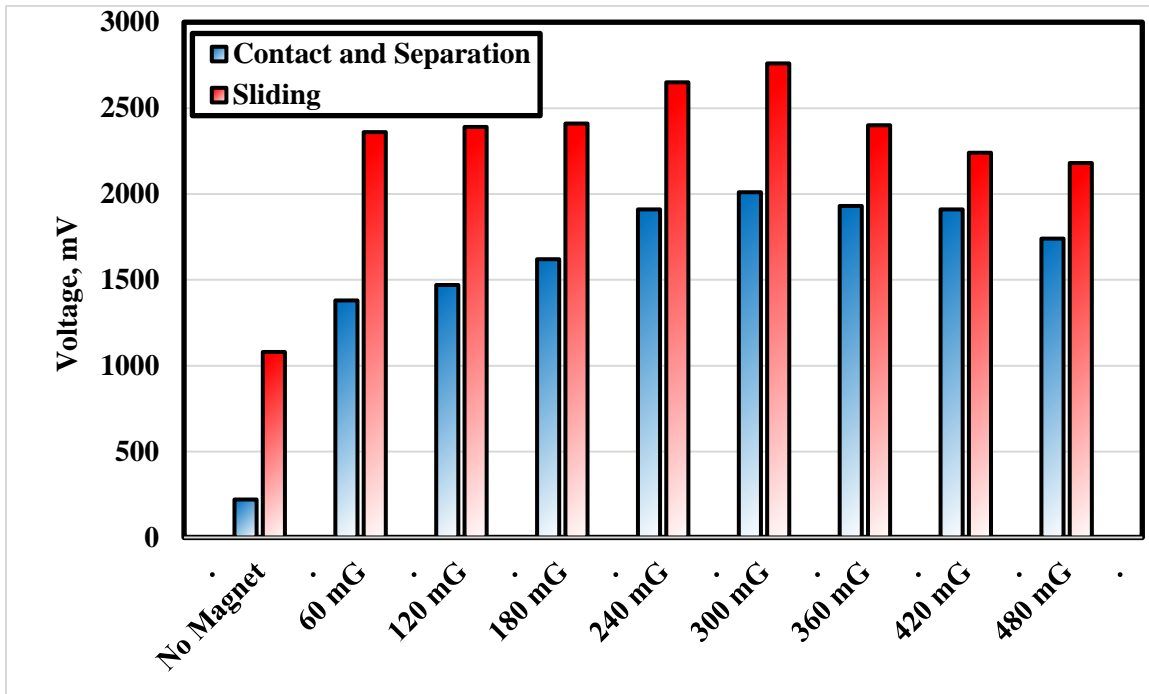


Fig. 7 Voltage generated from the contact-separation and sliding of PTFE on PA, where magnets are placed in the (IV) position.

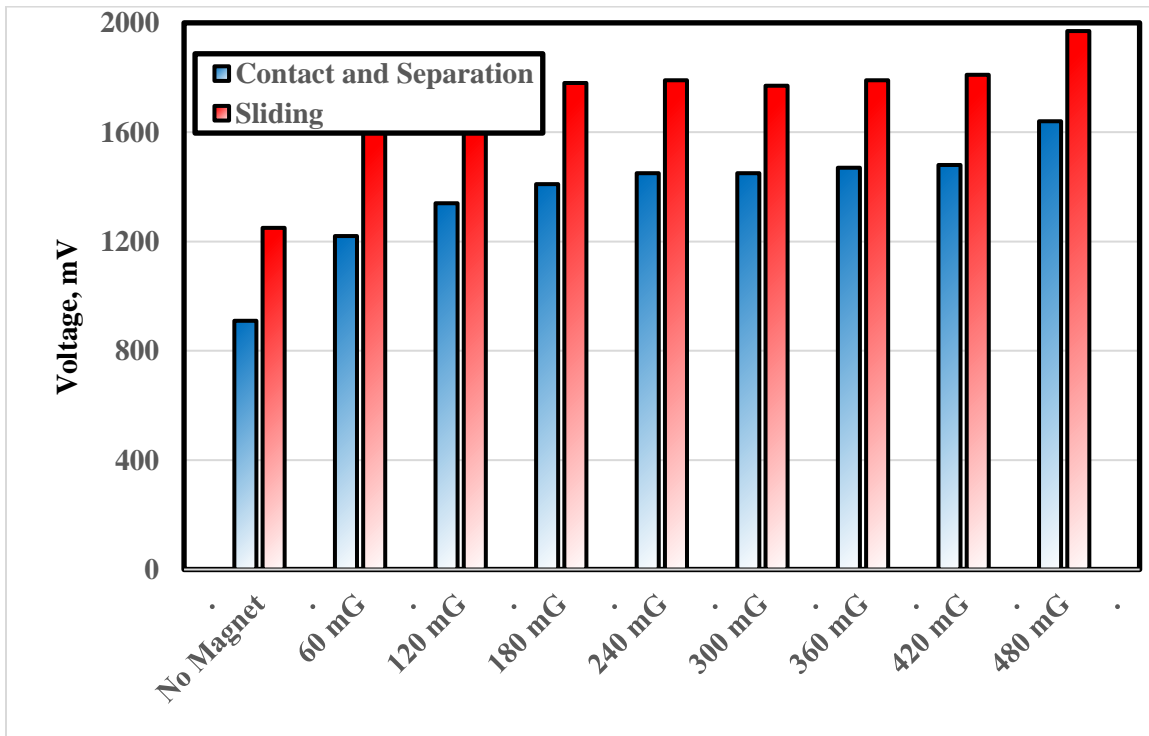
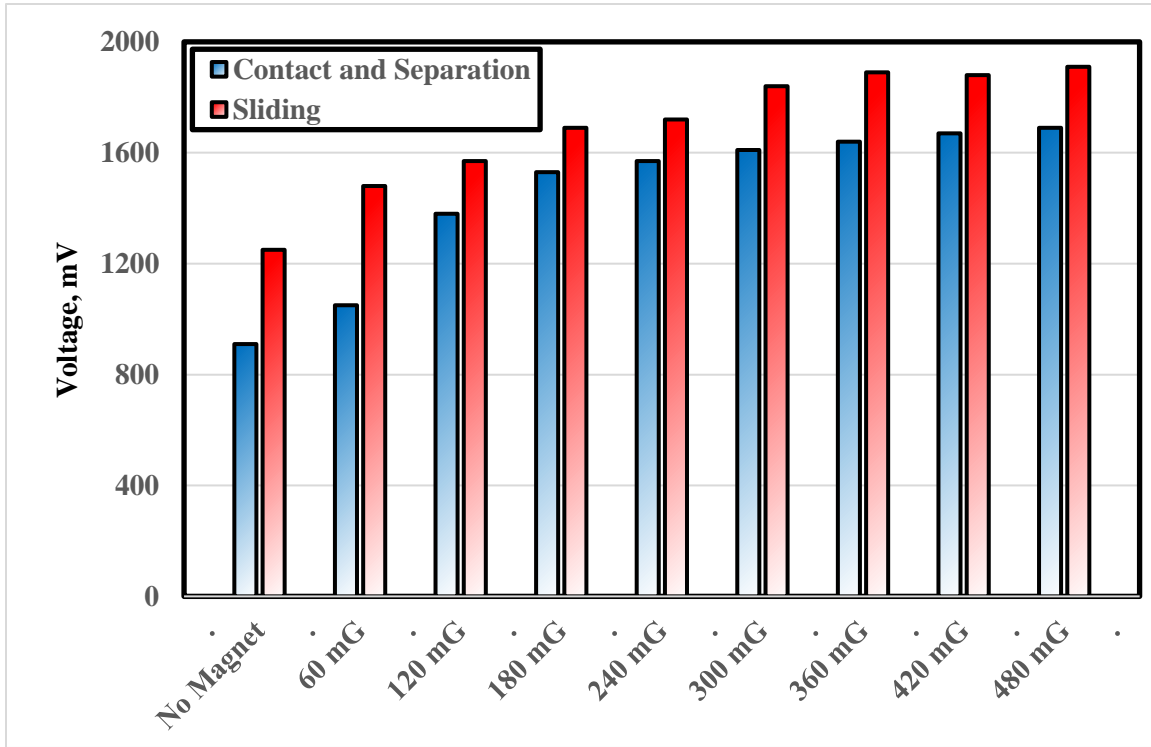
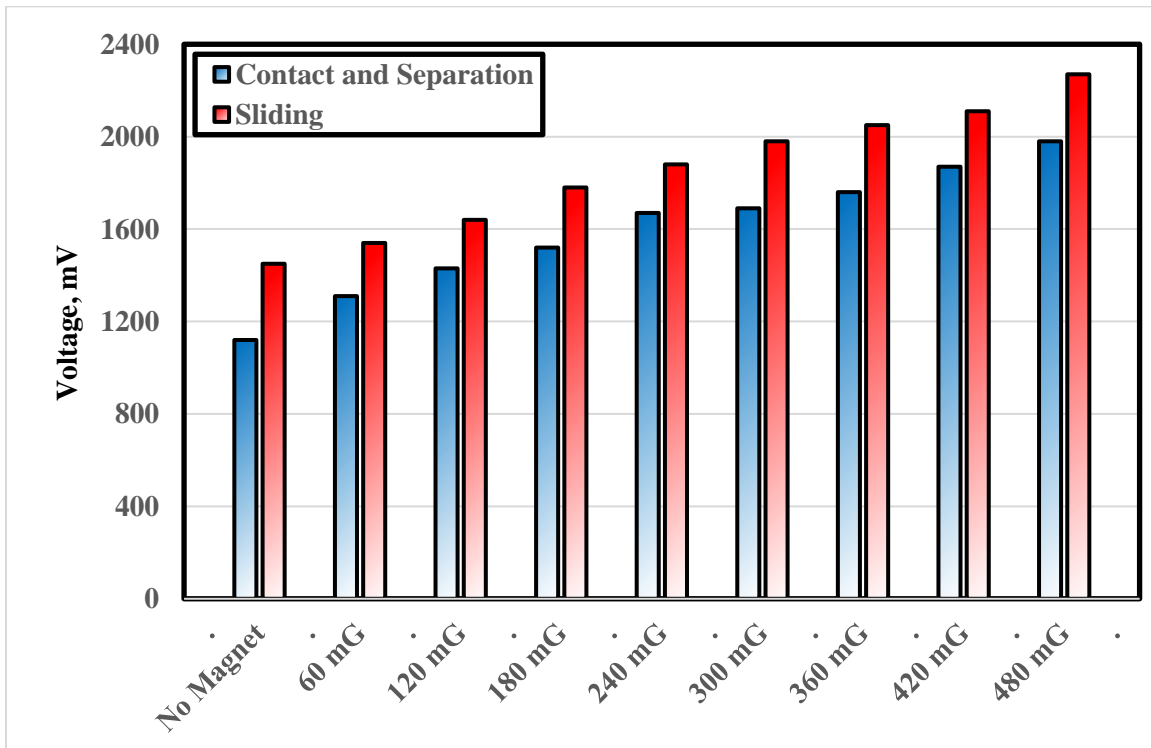


Fig. 8 Voltage generated from the contact-separation and sliding of rabbit fur on PP, where magnets are placed in the (I) position.



**Fig. 9 Voltage generated from the contact-separation and sliding of rabbit fur on PA, where magnets are placed in the (II) position.**



**Fig. 10 Voltage generated from the contact-separation and sliding of rabbit fur on PA, where magnets are placed in the (III) position.**

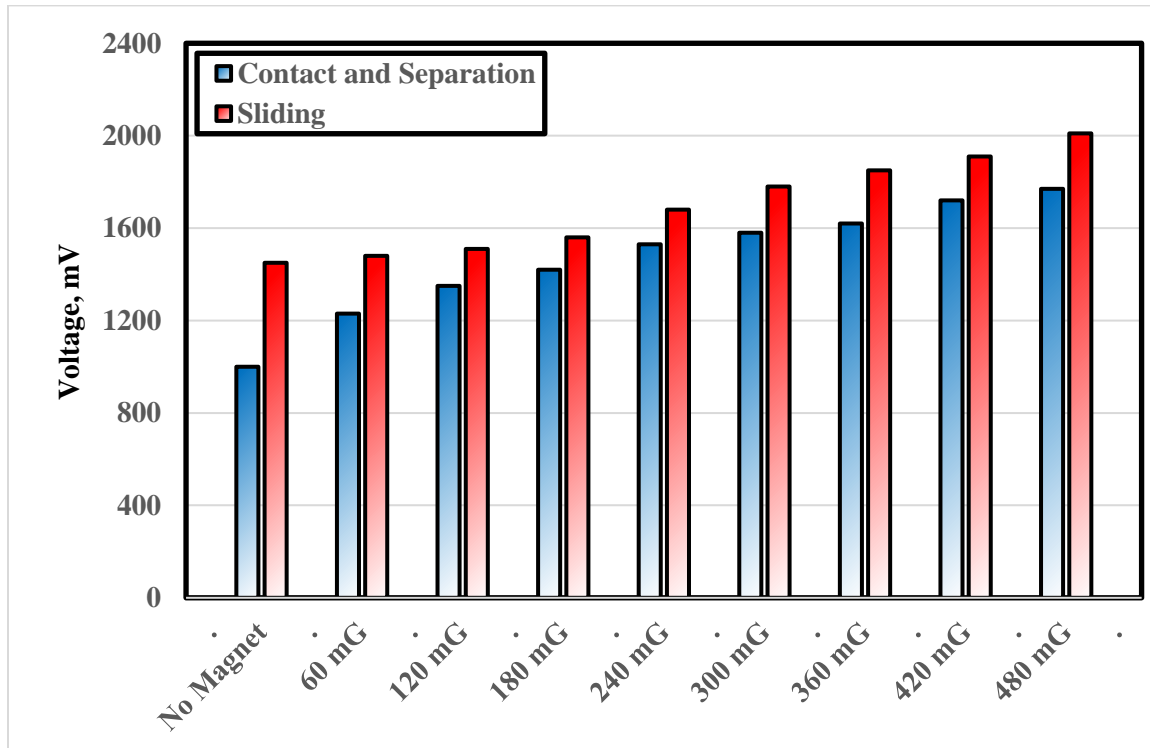


**Fig. 11 Voltage generated from the contact-separation and sliding of rabbit fur on PA, where magnets are placed in the (IV) position.**

The (III) position of the magnets relative to the sliding direction displayed relative higher voltage values generated from the contact-separation and sliding of PTFE on PA, Fig. 6. The voltage generated from contact-separation and sliding recorded 2060 and 2850 mV at 300 mG compared to that measured when the magnets were positioned as (I) and (II). That may be attributed to the increase of the number of the lines of the magnetic field cut by Al electrode of the first terminal. It seems that process would allow the Al electrode to cut more field lines. When the sliding was in the direction parallel to the field lines, (IV) position, Fig. 7, voltage recorded relatively lower values due to the decrease of the electromotive force that affected the generated voltage.

The effect of replacing the paper sheet by 0.12 mm thick PP sheet and the PTFE by rabbit fur on voltage generated from contact-separation and sliding is illustrated in Figs. 8 and 9. As expected, voltage values represented relatively higher values than that measured for paper sheet, Fig. 4. This is because the magnetic shielding in case of PP was lower than paper due to the variation of their thicknesses. The presence of PP of lower thickness allowed the lines of magnetic field to flow from one pole of the magnet to the other with the same intensity. As the thickness increased the field strength decreased. This fact will be examined carefully in further experiments. It is observed that the voltage significantly increased with increasing the strength of the magnetic field. The generated voltage represented relatively higher values than observed for that shielded by paper sheet. According to that observation, it is



recommended to use thinner materials as substrates in the design of the triboelectric nanogenerator. Voltage generated from the contact-separation and sliding of rabbit fur on PA, where magnets are placed in the (II) position displayed slight voltage decrease compared to condition of (II) position, Fig. 9, due to the decrease of the number of the magnetic field lines cut by the Al electrode.

When the magnets were placed in the (III) position, Fig. 10, higher values of voltage were measured because the magnets in that position allowed for the moving electrode to cut more field lines. It seems that the moving electrode induced electric and voltage. Like observed above the (IV) position generated lower voltage than (III) position, Fig. 11, due to the parallel movement of the electrode relative to the lines of the magnetic field.

## CONCLUSIONS

1. The optimal position of the magnets relative to the direction of sliding to get the highest voltage was determined when the moving electrode perpendicular cut the maximum number of the lines of the magnetic field.
2. When the substrate was paper sheet, voltage increased up to maximum then decreased with further increase of the field strength. The maximum voltage value was observed at 120 mG field strength. The voltage decrease with increasing magnetic fields may be from distribution of the magnets relative to the triboelectrified area.
3. Voltage increase was due to the movement of the Al electrode that perpendicular cut the lines of a magnetic field and induced an extra electric field leading to the voltage increase.
4. The sliding in the direction parallel to the field lines generated lower voltage values.
5. Voltage displayed relatively higher values for rabbit fur sliding on PP than that measured for PTFE sliding on PA.
6. It is recommended to select the proper position of the magnet to harvest the highest voltage values.

## REFERENCES

1. Al-Qaham Y., Mohamed M. K., and Ali W. Y., "Electric static charge generated from the friction of textiles", *Journal of the Egyptian Society of Tribology*, Vol. 10, No. 2, pp. 45 - 56, (2013).
2. Naik S., Mukherjee R., and Chaudhuri B., "Triboelectrification: A review of experimental and mechanistic modeling approaches with a special focus on pharmaceutical powders", *International journal of pharmaceutics*, Vol. 510, No. 1, pp. 375 - 385, (2016).
3. Lowell J., and Rose-Innes A., "Contact electrification", *Advances in Physics*, Vol. 29, No. 6, pp. 947 - 1023, (1980).
4. Badran A. H., Fouly A., Ali W. Y., and Ameer A. K., "Electrostatic Charges Generated on the Medical Clothes", *Journal of the Egyptian Society of Tribology*, Vol. 18, No. 2, pp. 15 - 26, (2021).
5. Ali A. S., "Triboelectrification of Synthetic Strings", *Journal of the Egyptian Society of Tribology*, Vol. 16, No. 2, pp. 26 - 36, (2019).
6. Zou H., Zhang Y., Guo L., Wang P., He X., Dai G., Zheng H., Chen C., Wang A. C., Xu C., et al., "Quantifying the triboelectric series", *Nature communications*, Vol. 10, No. 1, p. 1427, (2019).

7. Diaz A., and Felix-Navarro R., “A semi-quantitative tribo-electric series for polymeric materials: the influence of chemical structure and properties”, *Journal of Electrostatics*, Vol. 62, No. 4, pp. 277 - 290, (2004).
8. Burgo T. A., Galembeck F., and Pollack G. H., “Where is water in the triboelectric series?”, *Journal of Electrostatics*, Vol. 80, pp. 30 - 33, (2016).
9. McCarty L. S., and Whitesides G. M., “Electrostatic charging due to separation of ions at interfaces: contact electrification of ionic electrets”, *Angew. Chem. Int. Ed.*, Vol. 47, No. 12, pp. 2188 - 2207, (2008).
10. Gabor D., Radu S. M., Ghicioi E., Paraian M., Jurca A. M., Vatavu N., Paun F., and Popa C. M., “Study of methods for assessment of the ignition risk of dust/air explosive atmospheres by electrostatic discharge”, *Calitatea*, Vol. 20, No. S1, p. 93, (2019).
11. Glor M., and Thurnherr P., “Ignition Hazards Caused by Electrostatic Charges in Industrial Processes”, Thuba Ltd, (2015).
12. Von Pidoll U., “An overview of standards concerning unwanted electrostatic discharges”, *Journal of Electrostatics*, Vol. 67, No. 2-3, pp. 445 - 452, (2009).
13. Tian H., and Lee J. J., “Electrostatic discharge damage of MR heads”, *IEEE transactions on magnetics*, Vol. 31, No. 6, pp. 2624 - 2626, (1995).
14. Al-Kabbany A. M., and Ali W. Y., “Reducing the Electrostatic Charge of Polyester by Blending by Polyamide Strings”, *Journal of the Egyptian Society of Tribology*, Vol. 16, No. 4, pp. 36 - 44, (2019).
15. Ali A. S., Al-Kabbany A. M., Ali W. Y., and Samy A. M., “Reducing the Electrostatic Charge Generated from Sliding of Rubber on Polyethylene Artificial Turf”, *Journal of the Egyptian Society of Tribology*, Vol. 17, No. 2, pp. 40 - 49, (2020).
16. Ali A. S., El-Sherbiny Y. M., Ali W. Y., and Ibrahim R. A., “Selection of Floor Materials in Hospitals to Resist Covid-19”, *Journal of the Egyptian Society of Tribology*, Vol. 18, No. 1, pp. 40 - 51, (2021).
17. Ali A. S., Al-Kabbany A. M., Ali W. Y., and Badran A. H., “Triboelectrified Materials of Facemask to Resist Covid-19”, *Journal of the Egyptian Society of Tribology*, Vol. 18, No. 1, pp. 52 - 62, (2021).
18. Ali A. S., Al-Kabbany A. M., Ali W. Y., and Ibrahim R. A., “Proper Material Selection of Medical Safety Goggles”, *Journal of the Egyptian Society of Tribology*, Vol. 18, No. 2, pp. 1 - 14, (2021).
19. Al-Kabbany A. M., Ali W. Y., and Ali A. S., “Proposed Materials for Face Masks”, *Journal of the Egyptian Society of Tribology*, Vol. 18, No. 3, pp. 35 - 41, (2021).
20. Al-Kabbany A. M., Ali W. Y., and Ali A. S., “Proper Selection Materials of Face Shields, Eyeglasses and Goggles”, *Journal of the Egyptian Society of Tribology*, Vol. 18, No. 3, pp. 42 - 51, (2021).
21. Furfari F. A. “A history of the Van de Graaff generator”, *IEEE Industry Applications Magazine*, Vol. 11, No. 1, pp. 10–14, (2005).
22. Fan F.-R., Tian Z.-Q., and Wang Z. L., “Flexible triboelectric generator”, *Nano Energy*, Vol. 1, No. 2, pp. 328 - 334, (2012).
23. Goh Q. L., Chee P., Lim E. H., and Liew G. G., “Self-powered pressure sensor based on microfluidic triboelectric principle for human–machine interface applications”, *Smart Materials and Structures*, Vol. 30, No. 7, p. 075012, (2021).

24. Zhang R., Hummelgard M., Ortegren J., Olsen M., Andersson H., Yang Y., Olin H., and Wang Z. L., "Utilising the triboelectricity of the human body for human-computer interactions", *Nano Energy*, Vol. 100, , p. 107503, (2022).
25. Yang Y., Zhu G., Zhang H., Chen J., Zhong X., Lin Z.-H., Su Y., Bai P., Wen X., and Wang Z. L., "Triboelectric nanogenerator for harvesting wind energy and as self-powered wind vector sensor system", *ACS nano*, Vol. 7, No. 10, pp. 9461 - 9468, (2013).
26. Han J., Feng Y., Chen P., Liang X., Pang H., Jiang T., and Wang Z. L., "Wind-driven soft-contact rotary triboelectric nanogenerator based on rabbit fur with high performance and durability for smart farming", *Advanced Functional Materials*, Vol. 32, No. 2, p. 2108580, (2022).
27. Zhang H., Yang Y., Su Y., Chen J., Adams K., Lee S., Hu C., and Wang Z. L., "Triboelectric nanogenerator for harvesting vibration energy in full space and as self-powered acceleration sensor", *Advanced Functional Materials*, Vol. 24, No. 10, pp. 1401 - 1407, (2014).
28. Cheng P., Guo H., Wen Z., Zhang C., Yin X., Li X., Liu D., Song W., Sun X., Wang J., et al., "Largely enhanced triboelectric nanogenerator for efficient harvesting of water wave energy by soft contacted structure", *Nano Energy*, Vol. 57, pp. 432 - 439, (2019).
29. Meng B., Tang W., Too Z.-h., Zhang X., Han M., Liu W., and Zhang H., "A transparent single-friction-surface triboelectric generator and selfpowered touch sensor", *Energy & Environmental Science*, Vol. 6, No. 11, pp. 3235 - 3240, (2013).
30. Lei H., Xiao J., Chen Y., Jiang J., Xu R., Wen Z., Dong B., and Sun X., "Bamboo-inspired self-powered triboelectric sensor for touch sensing and sitting posture monitoring", *Nano Energy*, Vol. 91, p. 106670, (2022).
31. Pu X., Tang Q., Chen W., Huang Z., Liu G., Zeng Q., Chen J., Guo H., Xin L., and Hu C., "Flexible triboelectric 3D touch pad with unit subdivision structure for effective XY positioning and pressure sensing", *Nano Energy*, Vol. 76, p. 105047, (2020).
32. Haque R. I., Chandran O., Lani S., and Briand D., "Self-powered triboelectric touch sensor made of 3D printed materials", *Nano Energy*, Vol. 52, pp. 54 - 62, (2018).
33. Chen Y., Cheng Y., Jie Y., Cao X., Wang N., and Wang Z. L., "Energy harvesting and wireless power transmission by a hybridized electromagnetic-triboelectric nanogenerator", *Energy & Environmental Science*, Vol. 12, No. 9, pp. 2678 - 2684, (2019).
34. Quan T., Wang Z. L., and Yang Y., "A shared-electrode-based hybridized electromagnetic-triboelectric nanogenerator", *ACS Applied Materials & Interfaces*, Vol. 8, No. 30, pp. 19 573 - 19 578, (2016).
35. Qin K., Chen C., Pu X., Tang Q., He W., Liu Y., Zeng Q., Liu G., Guo H., and Hu C., "Magnetic array assisted triboelectric nanogenerator sensor for real-time gesture interaction", *Nano-micro letters*, Vol. 13, pp. 1 - 9, (2021).
36. Ali A. S., Al-Kabbany A. M., and Ali W. Y., "Voltage Generated From Triboelectrification of Rabbit Fur and Polymeric Materials", *Journal of the Egyptian Society of Tribology*, Vol. 19, No. 3, pp. 10 - 18, (2022).
37. Zhang R., and Olin H., "Material choices for triboelectric nanogenerators: a critical review", *EcoMat*, Vol. 2, No. 4, p. e12062, (2020).
38. Ali A. S., Youssef M. M., Ali W. Y. and Elzayady N., "Triboelectric Nanogenerator Based on Contact and Separation as well as Sliding of Polyamide on Polytetrafluoroethylene", *Journal of the Egyptian Society of Tribology*, Vol. 20, No. 1, January 2023, pp. 32 – 40, (2023).

- 39. Ali A. S., Youssef M. M., Ali W. Y. and Rashed A., “Enhancing the Efficiency of Triboelectric Nanogenerator by Electrostatic Induction”, Journal of the Egyptian Society of Tribology, Vol. 20, No. 1, January 2023, pp. 41 – 50, (2023).**
- 40. Ali A. S., Youssef M. M., Ali W. Y. and Elzayady N., “Performance of Triboelectric Nanogenerator Enhanced by Electrostatic Induction”, Journal of the Egyptian Society of Tribology, Vol. 20, No. 2, April 2023, pp. 13 – 22, (2023).**
- 41. Ali A. S., Youssef M. M., Ali W. Y. and Rashed A., “Triboelectric Nanogenerator Based on Triboelectrification and Magnetic Field”, Journal of the Egyptian Society of Tribology, Vol. 20, No. 2, April 2023, pp. 1 – 12, (2023).**